Multimode non-classical light generation through the OPO threshold

Benoît Chalopin, Francesco Scazza, Claude Fabre, Nicolas Treps

Multimode non-classical light generation through the OPO threshold

B. Chalopin,[1,*] F. Scazza,[1] C. Fabre,[1] and N. Treps[1]

[1] *Laboratoire Kastler Brossel, Université Pierre et Marie-Curie-Paris 6, ENS, CNRS ; 4 place Jussieu, 75005 Paris, France*

(Dated: December 21, 2009)

We show that an Optical Parametric Oscillator which is simultaneously resonant for several modes, either spatial or temporal, generates both below and above threshold a multimode non-classical state of light consisting of squeezed vacuum states in all the non-oscillating modes. We confirm this prediction by an experiment dealing with the degenerate TEM_{01} and TEM_{10} modes. We show the conservation of non-classical properties when the threshold is crossed. The experiment is made possible by the implementation of a new method to lock the relative phase of the pump and the injected beam.

PACS numbers:

Optical parametric oscillators are among the best generators of non-classical states of light. Below the oscillation threshold, they have been shown to generate squeezed vacuum states [1] and bi-partite entangled states. Above the oscillation threshold, they generate intensity correlated twin beams [2], squeezed reflected pump [3], bright bi-partite [4] or tri-partite [5] entangled states. Very impressive amounts of squeezing (11dB) have been recently observed below threshold[6]. Experimental results are less spectacular above threshold, because of the detrimental effect of the pump beam excess noise. Generally speaking, the non-classical properties increase when one approaches from below or from above the oscillation threshold, or any other bifurcation point of the non-linear dynamics of the device[7, 8], but it is not always the case: for instance the signal-idler intensity difference squeezing is independent of the pumping level. This property of "non-critially squeezed light" has been further explored by the Valencia group[10] in the context of quantum imaging, which has found other squeezing effects that are independent of the pumping level. These effects are related to spatial symmetry-breaking, either translational[9] or rotational[10]: in a cavity of cylindrical symmetry, the parametric gain is the same for Gaussian modes TEM_{01} where the two lobes are aligned along any direction in the transverse plane. However, above the oscillation threshold, a unique TEM_{01} mode is produced. It is shown that this spontaneous symmetry breaking "induces" the generation of a squeezed vacuum state in the mode orthogonal to the emitted one with a squeezed value independent of the pumping level and clamped to its value at threshold. The emitted field is thus a two-mode non-classical field, made of the superposition of a bright mode and a vacuum-squeezed mode.

In this paper, we show theoretically that this important result can be generalized to a much wider class of situations, involving either spatial or temporal modes, and we check experimentally that one can efficiently produce in this way multimode non-classical light.

Let us envision the situation in which the cavity of the OPO is simultaneously resonant on several modes, which can be either spatial modes (Hermite-Gauss modes or more complicated patterns in transverse degenerate cavities), or frequency modes (separated by the free spectral range of the cavity). The annihilation operators $\hat{a}_\ell$ associated with these different modes and the pump mode operator $\hat{b}$ obey then the following well-known evolution equations, describing the effect of the parametric splitting of pump photons into couples of signal and idler photons respectively in modes ℓ and ℓ'

$$\tau \frac{d}{dt}\hat{a}_\ell = -\gamma \hat{a}_\ell + \sum_{\ell'} G_{\ell,\ell'} \hat{b} \hat{a}^\dagger_{\ell'} + \sqrt{2\gamma}\hat{a}^{in}_\ell \qquad (1)$$

assuming equal cavity losses γ for all the modes ℓ. τ is the cavity round-trip time. The pump is described by a single mode $\hat{b}$ having a well-defined spatial and temporal variation. $\hat{a}^{in}_\ell$ are the input modes. Like in [11], we take into account the fact that the parametric coupling coefficients $G_{\ell,\ell'}$ between the signal modes and the pump vary according to the strength of the overlap between the modes $\hat{a}_\ell$, $\hat{a}_{\ell'}$ and $\hat{b}$. $G_{\ell,\ell'}$ is a symmetric matrix which can always be diagonalized: let us call Λ_k its real eigenvalues. The corresponding eigenvectors are "supermodes"[12, 13, 14], associated to annihilation operators $\hat{S}_k$, which obey the following decoupled equations:

$$\tau \frac{d}{dt}\hat{S}_k = -\gamma \hat{S}_k + \Lambda_k \hat{b} \hat{S}^\dagger_k + \sqrt{2\gamma}\hat{S}^{in}_k \qquad (2)$$

The mean intensity of the different supermodes $\hat{S}_k$ is zero as long as the system stays below threshold. Let us call $\hat{S}_1$ the supermode associated to the eigenvalue Λ_1 of highest modulus (in the situation studied in [10], this eigenvalue is degenerate, because of symmetries in the considered device). When one increases the pump power, this mode will reach first the oscillation threshold. It is easy to show that below this threshold all these modes are in squeezed vacuum states, the squeezing increasing when one approaches the threshold. At threshold, the noise on the squeezed quadrature has a variance at zero noise fre-

quency $V_{k,min}$ (normalized to vacuum noise) equal to[12]:

$$V_{k,min} = \left(\frac{|\Lambda_k| - |\Lambda_1|}{|\Lambda_k| + |\Lambda_1|} \right)^2 \quad (3)$$

meaning that all modes with eigenvalues equal to Λ_1 or $-\Lambda_1$ are perfectly squeezed. This property has been recently checked experimentally in the case of a cavity with cylindrical symmetry by two groups[15, 16], which have demonstrated simultaneous squeezing on two orthogonal first-order hermite gaussian modes TEM_{10} and TEM_{01} produced by a degenerate OPO pumped by a TEM_{00} below the oscillation threshold.

Let us now consider the above threshold case, but close enough to the threshold so that one can neglect the distortion of the pump mode shape inside the crystal due to pump depletion. The first supermode $k = 1$ oscillates and the intracavity pump mode has a nonzero mean value $\left\langle \hat{b} \right\rangle$ "clamped" at a value γ/Λ_1, or $-\gamma/\Lambda_1$, independent of the pump input intensity. The others are still below threshold and have zero mean values. The evolution equations of these modes are obtained by the usual procedure of linearization of operators equations around the mean values. One gets:

$$\tau \frac{d}{dt} \hat{S}_k = -\gamma \hat{S}_k \pm \gamma \frac{\Lambda_k}{\Lambda_1} \hat{S}_k^\dagger + \sqrt{2\gamma} \hat{S}_{in,k} \quad (k \neq 1) \quad (4)$$

from which one easily derives that all these modes are also "clamped" to the squeezed vacuum state that they had reached when approaching the threshold from below, as long as pump depletion does not distort significantly the pump mode shape. Their minimum variance is then given by Eq.(3) whatever the pump power. All modes for which $|\Lambda_k| \simeq |\Lambda_1|$ are therefore significantly squeezed. We have thus shown that *an OPO simultaneously resonant on different modes produces above threshold a multimode nonclassical state consisting of several squeezed vacuum superposed to a bright mode.*

The principle of our experiment is shown on Fig. 1. The OPO cavity is pumped by a TEM_{00} mode and the cavity is simultaneously resonant for the two transverse modes TEM_{10} and TEM_{01}. The mode matching properties of our device are such that the lowest oscillation threshold is obtained for a couple of non frequency degenerate signal and idler modes both in a transverse TEM_{00} mode. Consequently, the two frequency degenerate EM_{10} and TEM_{01} transverse modes, having a higher threshold, should be in a squeezed vacuum state, both below and above the oscillation threshold. This is what we want to check in the experiment

The experimental setup is depicted on Fig. 2. We build a two-mode degenerate OPO exploiting the simultaneous resonance of both TEM_{10} and TEM_{01} in a linear cavity, and we placed a $1mm \times 2mm \times 10mm$PPKTP non-linear crystal inside. The high non-linear efficiency of the PPKTP enables us to use a single-pass $532nm$ pump beam

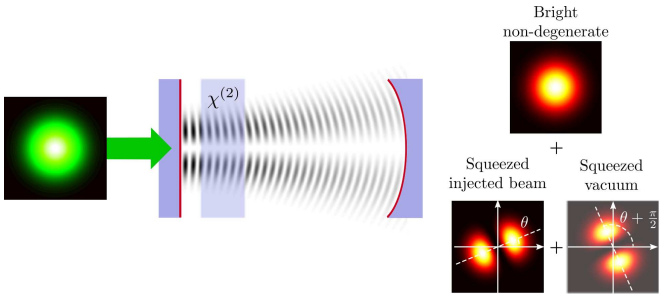

FIG. 1: Principle of the squeezing generation in a degenerate OPO above threshold

from a frequency-doubled $1064nm$ YAG laser. The input coupler is a highly reflective plane mirror at $1064nm$ with $R = 99.8\%$ and the output coupler is a spherical mirror of radius of curvature $50mm$ and reflectivity $R = 98.3\%$. The intra-cavity losses are around 0.2% and are mainly due to the non-linear crystal. The cavity finesse is $\mathcal{F} = 300$ with an escape efficiency of 80%. This value is a trade-off between the level of squeezing we can observe with this OPO and the power of the pump at the threshold of the OPO. The cavity length is $47mm$ and results in a bandwidth of $11MHz$.

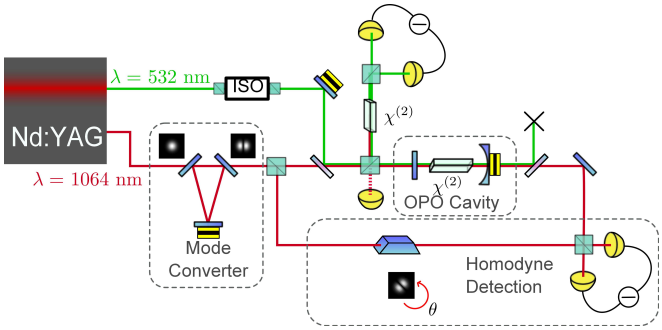

FIG. 2: Schematics of the experimental setup

We generate a horizontal TEM_{10} mode with a mode converter cavity (MC) seeded with a misaligned TEM_{00}. This mode is seeded in the OPO cavity to achieve alignment and locking at resonance. The pump is a TEM_{00} mode. Its mode-matching is a delicate operation: as reported in [17], the optimal pump profile for the amplification of a TEM_{10} and a TEM_{01} would be a combination of TEM_{00}, TEM_{20} and TEM_{02}. For simplicity reasons, we chose to use a TEM_{00} mode only, whose waist is ajusted to maximize the amplification gain of both the TEM_{10} and the TEM_{01}. The degeneracy of the cavity for these two modes is easy to obtain when the cavity is empty. The periodic poling of the PPKTP crystal induces a slight disymmetry, which makes the cavity non-degenerate, but can be compensated with a fine tuning of the crystal temperature.

To keep the OPO stable while crossing the oscillation

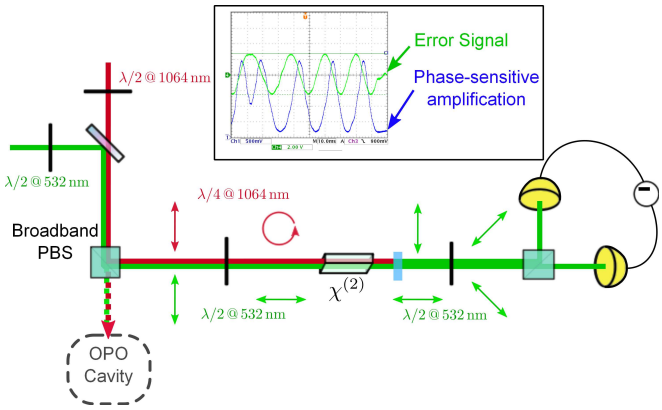

FIG. 3: Error signal generation for the relative phase between OPO seed and pump beams. Polarisations of the beams, as shown on the figure, are choosen to allow interferences only on the last beamsplitter. The phase-sensitive amplification and the error signal (windowed) show perfect correlation.

threshold, and continuously compare the two regimes, one must perform all the necessary lockings on the beams upstream from the cavity. The cavity length is locked at resonance using the Pound-Drever-Hall technique [18]. When the cavity is locked on a TEM_{00} resonance, the pump threshold is $250mW$, while for the TEM_{10} resonance the threshold becomes $450mW$. The relative phase between the seed and the pump of the OPO has to be locked in the de-amplification regime in order to observe amplitude squeezing. To this end, an error signal is generated independently of the OPO with a technique depicted on Fig 3. An interferometer is built between the input pump and the seed frequency doubled within a PPKTP crystal. Since the optical path is identical for all the modes, the interference between the pump and the frequency doubled seed, that depends on the two intensities and the relative phase ϕ between the pump beam and the seed of the OPO, can be used as an error signal.

$$s(\phi) \propto \sqrt{I_{\text{pump}}} I_{\text{seed}} \cos(2\phi - \phi_0) \qquad (5)$$

where ϕ_0 is an offset phase, that can be tuned simply by moving the crystal longitudinally in order to lock the relative phase ϕ. The key points for this non-linear interferometer are on the one hand to use a broadband polarizing beamsplitter which enables us to independently tune the powers of the two beams sent in the interferometer, and on the other hand the high non-linear coefficient of the PPKTP that makes possible the single pass frequency doubling of an infrared beam with a sufficient efficiency. The locking turned out to be very stable once the two relative powers sent inside the interferometers have been carefully chosen. In our case, we sent about $30mW$ of infrared power and less than $1mW$ of green power.

The quantum state of the output modes of the OPO

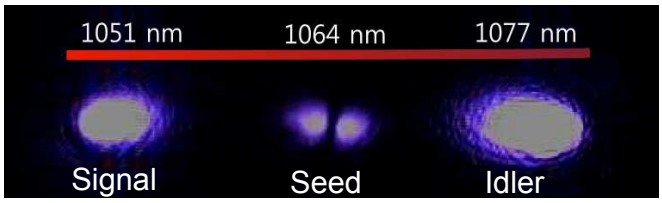

FIG. 4: Wavelength measurement of the signal and idler beams emitted in a TEM_{00} mode when the OPO is seeded with a TEM_{10} at $1064nm$.

is analyzed with a homodyne detection. The local oscillator is a TEM_{10} of arbitrary orientation, generated by rotating the mode transmitted by the MC with a Dove prism [16]. It is first aligned when the mode converter is locked on the TEM_{00} with a visibility above 98%, so that the orthogonality of the eigenmodes of the MC assures the orthogonality of the ones measured with the homodyne detection. Below the threshold, the output of the OPO shows multimode squeezing on both the injected TEM_{10} and the vacuum TEM_{01} modes with 20% noise reduction ($1dB$). The system has more losses and smaller bandwidth than OPOs optimized for squeezing which explains the low amount of squeezing. This value has to be compared with the squeezing observed in the same experimental conditions on a TEM_{00} mode, which is $1.5dB$. The ratio between squeezing on these two modes is in agreement with the prediction of Eq.(3), as the coupling coefficient between pump and TEM_{01} is 0.64 times smaller than the coupling between pump and TEM_{00}.

The lockings of the cavity length and the relative phase being independent from the OPO, we can investigate the quantum behaviour of the output modes through the oscillation threshold. In our case, when locked on the TEM_{10} at $1064nm$, the transverse mode emitted by the OPO above threshold depends on the mode-matching of the pump. We chose to have it emit a couple of frequency non-degenerate signal and idler TEM_{00}. This is possible thanks to the very large phase-matching curves of the PPKTP crystal. Using a diffraction grating we measured the frequency of the TEM_{00} signal and idler modes and found $\lambda = 1051nm$ and $1077nm$ as shown on Fig. 4. This value agrees with the theoretical prediction taking into account the dispersion inside the PPKTP crystal [19], and the value of the Gouy Phase of the gaussian modes inside the cavity.

The same homodyne detection as described before is used to investigate the multimode behavior of the output of the OPO above threshold. The results follow the predictions of the theoretical part of the present paper and we observed multimode squeezing with an amount of squeezing independaent from the pump intensity. The results are first shown on Fig. 5 when crossing the oscillation threshold, and on Fig. 6 further above when the TEM_{00} emission is bright, around $3mW$ of power. For

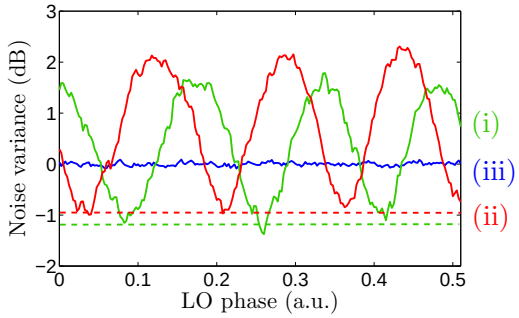

FIG. 5: Squeezing measured on the TEM_{01} vacuum mode at the oscillation threshold of the OPO. The green curve (i) is just below the threshold, whereas the red curve (ii) is just above. We observe in both cases $1 \pm 0.2dB$ of squeezing. The anti-squeezing on the orthogonal quadrature is increased at the threshold, from $1.7 \pm 0.2dB$ to $2 \pm 0.2dB$.

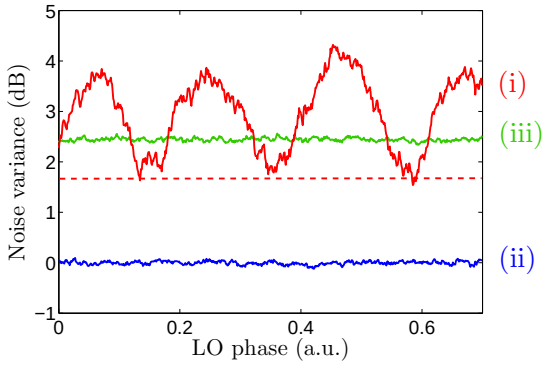

FIG. 6: Squeezing measured on the TEM_{10} seed mode above the oscillation threshold of the OPO. The red curve (i) represents the measured noise, the blue curve (ii) the noise of the local oscillator, and the green curve (iii) represents the shot noise defined as a corrected value of the shot noise taking into account the bright emission. For several pump powers, we observe $1 \pm 0.3dB$ of squeezing and $2 \pm 0.3dB$ of anti-squeezing.

different pump powers, we measured $1dB$ of squeezing and $2dB$ of anti-squeezing on the two transverse modes, which is the same as below the threshold. When the TEM_{00} emission is bright, we have to correct the value of the shot noise measured with the local oscillator alone, because the homodyne detection photodiodes measures the bright emission as well as the low-power TEM_{10} and the vacuum TEM_{01}.

We characterized that the state produced by the OPO above the oscillation threshold is an intrinsic tri-mode state, as defined by [20]. Using the most simple multimode OPO, we generated and characterized a beam in which the energy is carried by one mode, and two orthogonal modes carried non-classical features. This demonstration of the pump clamping inside OPOs sets a new regime within easy reach of the experimentalists to produce multimode non-classical states and for which the squeezing is independent from the pump power. Moreover, the multimode features of the OPO are preserved above the oscillation threshold. This device is thus a potential stabilized source for quantum information protocols in the continuous wave regime. Highly multimode operation can be potentially performed using the synchronously pumped OPO described in [12] or the OPO in a self-imaging cavity described in [14].

We would like to thank German de Valcarcel and Hans-A. Bachor for fruitful discussions. We acknowledge the financial support of the Future and Emerging Technologies (FET) programme within the Seventh Framework Programme for Research of the European Commission, under the FET-Open grant agreement HIDEAS, number FP7-ICT-221906

* Electronic address: chalopin@spectro.jussieu.fr

[1] L.A. Wu, H.J. Kimble, J.L. Hall and H. Wu, Phys. Rev. Lett. **57**, 2520 (1986)
[2] A. Heidmann, R. J. Horowicz, S. Reynaud, E. Giacobino, and C. Fabre, Phys. Rev. Lett. **59**, 2555 (1987)
[3] K. Kasai, Gao Jiangrui, C. Fabre, Europhysics Lett. **40**, 25 (1997)
[4] Z. Y. Ou, S. Pereira, H. J. Kimble, K. C. Peng, Phys. Rev. Lett. **68**, 3663 (1992)
[5] A. Coelho, F. Barbosa,1 K. Cassemiro, A. Villar, M. Martinelli, P. Nussenzveig, Sciencexpress, 10.1126/science.1178683 (2009)
[6] H. Vahlbruch, M. Mehmet, N. Lastzka, B. Hage, S. Chelkowski, A. Franzen, S. Gossler, K. Danzmann, R. Schnabel, Phys. Rev. Lett. **100**, 033602 (2008)
[7] C. Fabre, Physics Reports **219**, 215 (1992)
[8] L. Lugiato, P. Galatola, L. Narducci, Optics Commun. **76**, 276 (1990)
[9] I. Pérez-Arjona, E. Roldan and G.J. Valcarcel, Euroohys. Lett. (2006) **74** 247 (2006)
[10] C. NavarreteBenlloch, E. Roldan, and G.J. de Valcarcel, Phys. Rev. Lett. **100**, 203601 (2008)
[11] C. Navarrete-Benlloch, G.J. de Valcarcel and E. Roldán, Phys Rev A **79** 043820 (2009)
[12] G.J. de Valcarcel, G. Patera, N. Treps and C. Fabre, Phys. Rev. A **74**, 061801(R) (2006)
[13] G. Patera, G.J. de Valcarcel, N. Treps and C. Fabre, to be published in Eu. Phys. Journal D (2009)
[14] L. Lopez, B. Chalopin, A. Rivière de la Souchère, C. Fabre, A. Maître, and N. Treps, Phys. Rev. A **80**, 043816 (2009)
[15] M. Lassen, G. Leuchs, and U.L. Andersen, Phys. Rev. Lett. **102** 163602 (2009)

[16] J. Janousek, K. Wagner, J.F. Morizur, N. Treps, P.K. Lam, C.C. Harb, and H.A. Bachor, Nature Photonics **3** 399 (2009)
[17] M. Lassen, V. Delaubert, C. Harb, P.K. Lam, N. Treps, and H.A. Bachor, JEOS RP **1** 06003 (2006)
[18] R.W.P. Drever, J.L. Hall, F.V. Kowalski, J. Hough, G.M. Ford, A.J. Munley, and H. Ward, Appl. Phys. B **31** 97 (1983)
[19] K. Fradkin, A. Arie, A. Skliar, and G. Rosenman, Appl. Phys. lett., **74** 914 (1999)
[20] N. Treps, V. Delaubert, A. Maître, J.M. Courty, and C. Fabre, Phys. Rev. A **71** 013820 (2005)